Geometry, Material Properties and Bond Performance of Prototype Titanium Reinforcing Bars

Shawn Platt[1] and Kent A. Harries[2,3]

Abstract

The use of titanium as a concrete reinforcing bar material has been proposed. This study summarizes measured geometric and experimentally determined material properties of 6Al-4V titanium reinforcing bars and comparable properties of ASTM A615 steel. All bars are nominally #5 bars. Bond characteristics of the titanium bars were assessed through ASTM D7913 pull-out tests, ASTM A944 beam-end tests and four concrete prism tension tests. The nature of reinforcing bar bond to concrete is such that deformed bars exhibit very similar patterns of bond stress-slip behaviour. Provided adequate deformations are provided, the bond-slip relationship is dominated by concrete behaviour. The bond performance of the 6Al-4V titanium bars was similar to that of A615 steel bars and, as expected, clearly affected by the rib ratio. The results presented reinforce the ASTM A615-implied lower limit for the rib ratio, $R_r > 0.05$. The implication of a similar bond-stress behaviour is that existing bond relationships for steel-reinforced concrete likely apply to titanium bars provided they meet the deformation requirements of ASTM A615 – the standard for which steel reinforcing bars, and therefore their bond characterisation – is calibrated. Both the pull-out and beam-end test results reinforce the conclusion that bond behaviour of titanium bars is essentially the same as that steel bars. The bond stresses, normalised to account for variation in concrete strength, are similar and the calculated development lengths are essentially in the ratio of yield strengths of the materials. The prism tension tests demonstrated that concrete crack width is proportional to modular ratio of the reinforcing material, while spacing is inversely proportional to the stiffness of the initial bond-slip response.

Keywords: bond; concrete; reinforcing bars; titanium

---

[1] Post-doctoral Fellow, University of Bath; formerly PhD candidate, University of Pittsburgh

[2] Bicentennial Board of Visitors Faculty Fellow and Professor, University of Pittsburgh, kharries@pitt.edu

[3] Leverhulme Visiting Professor, University of Bath

Introduction

Titanium bars for concrete reinforcement have been proposed (Adkins and George 2017); their use for structural rehabilitation have been demonstrated in laboratory tests and in a single field application (Higgins et al. 2015 and 2017). The demonstrated application was the near-surface mounting (NSM) of titanium 'staples' – straight bars having a 90 degree bend at either end to affect anchorage. The #5 (16 mm diameter) titanium bars used had machined thread-like deformations. The primary advantage of titanium over steel in this application is its corrosion resistance permitting the reduced cover inherent in an NSM repair. The 6Al-4V titanium described in this paper, is a material exhibiting high strength and ductility. Titanium also exhibits high toughness and resistance to damage, and maintains a high maximum service temperature (Adkins and George 2017) making it a promising material for reinforcing concrete (Higgins 2015). The present paper is part of a large study investigating specific aspects of the use of titanium as a concrete reinforcing material (Platt 2018).

Titanium as Concrete Reinforcement

The stress-strain and other fundamental material behaviours of the 6Al-4V titanium (UNS designation R56400) bars used in this study are similar in form to those of steel. Like steel, 6Al-4V titanium exhibits an elastic behaviour to a proportional limit, a definable yield value followed by some degree of strain hardening, and exhibits a great deal of ductility. The 6Al-4V titanium exhibits yield strength approximately twice that of ASTM A615 reinforcing steel and an extensional modulus about 55% of steel. Thus, the yield strain of 6Al-4V titanium is on the order of 0.008, approximately four times greater than A615 steel. The material properties of 6Al-4V titanium is both an advantage and a disadvantage when considering titanium as an alternative to steel reinforcement. It is an advantage in the sense that engineers are comfortable with the behaviour profile of the material. For applications in which only the ultimate capacity of reinforcement is a concern, approximately half the reinforcement volume is required where titanium used in place of steel; this may ease placement of reinforcement and reduce congestion. The softer response, however, affects the assumed reinforced concrete behaviour and can be a disadvantage when considering serviceability (crack spacing and width, and deflections) or other concrete

performance parameters such as ensuring aggregate interlock. The behaviour of concrete reinforcing bars, particularly under service loads, is a function of axial stiffness, *EA* (the product of modulus and cross sectional area). Thus to directly replace steel with titanium, twice as much titanium as steel is required; resulting in greater congestion. To reduce the amount of titanium reinforcement required, the alternative design paradigm used for glass fibre-reinforced polymer (GFRP) reinforcing bars (ACI 440.1R) – whose behaviour is elastic to failure and whose modulus ranges from 20% to 50% that of steel – may be appropriate for titanium-reinforced concrete; a comparison of design paradigms is presented in Platt (2018).

Nevertheless, the titanium staples demonstrated by Higgins et al. (2015 and 2017) exhibited a few potential drawbacks: firstly, the 6Al-4V titanium bars used had small machined thread-like deformations that had relatively poor bond performance in concrete (mortar 'clogged' the small threads resulting in little mechanical bond). Such bars provide limited crack control over their length rendering long staple applications inefficient under serviceability conditions. Secondly, titanium must be bent at controlled temperatures on the order of 500^{o}C adding fabrication cost and making field-bends impractical. Titanium bars having rolled deformations more typical of steel reinforcing bars potentially overcome both concerns: a) appropriate deformations provide uniform bond over the length of the bar which b) can also be used to provide conventional development length anchorage of straight bars.

It is proposed that titanium reinforcing bars may have a market in concrete and masonry repair applications (Adkins and George 2017), particularly in unique environments and in connection with historic structures since titanium is noncorroding and mostly otherwise inert. Nonetheless a number of performance parameters in relation to titanium reinforcing bars and their integration into new or existing construction remain. Platt and Harries (2018) concluded that, despite a galvanic potential of approximately 0.65V, there was no evidence that 6Al-4V titanium bars (cathode) in close proximity to steel bars (anode) in concrete affected corrosion rates of the steel. The galvanic corrosion behaviour of A615 steel and 6Al-4V titanium bars were statistically no different than A615 bars coupled with wither stainless steel or carbon fibre bars (both commonly accepted in concrete construction). This paper reports

a study of the bond characterisation of deformed 6Al-4V titanium reinforcing bars in addition to summarising fundamental geometric and material properties of the prototype rolled deformed bars.

Bond Characterisation of Titanium Reinforcing Bars

In a reinforced concrete member, internal equilibrium is achieved as the tension force carried by the reinforcement balances the compression force carried by the concrete. The tension force is transferred to the reinforcement through bond between the reinforcement and concrete into which it is embedded. Bond stresses exist whenever the force in the tensile reinforcement changes. With the exception of unbonded post-tensioned concrete members, design assumptions (e.g., ACI 318) assume conditions of "perfect bond" through the developed yield stress in the reinforcing. This assumption, implies that strain compatibility is enforced over the entire member and equilibrium is maintained locally at cracks.

Bond is developed by chemical adhesion, friction, and mechanical interlock between bar deformations and the surrounding concrete. Adhesion is small, rapidly overcome and therefore neglected. The remaining components form a resultant stress that can be further broken into longitudinal and radial components. For deformed bars, mechanical interlock is the primary method of bond force transfer. Bond of reinforcing steel is conventionally assessed using 'pull-out' tests having short embedment lengths (ASTM D7913 and similar). Such tests are not appropriate for determining characteristic development lengths and behaviour, particularly for non-conventional reinforcing bar geometries; full development length tests such as 'beam-end' tests are required for this purpose (ASTM A944 and similar).

The bond mechanism depends on a number of factors including bar size, shape, deformation geometry and elastic modulus. Bond capacity is additionally dependent upon confining concrete strength and the effects of confining reinforcement, if present. When considering titanium reinforcing bars, two issues associated with bond arise:

1. The deformations provided may substantially differ in geometry from those used on conventional reinforcing steel (assumed in this paper to be compliant with ASTM A615 reinforcing bars) resulting in a different stress transfer mechanism and therefore a different capacity.

2. The lower modulus of titanium as compared with steel requires larger strains to develop the same reinforcing stress (by a factor of approximately two) and larger strains still (factor of approximately four) to effectively develop the capacity of the bar. Our present understanding of bond to concrete does not typically consider these larger strains.

Rather than address bond stress directly, reinforced concrete design uses the concept of development length. The development length, l_d, is the length of embedment required for the bar stress to increase from zero to the yield strength, f_y; i.e., to fully 'develop' the bar capacity. If the development is inadequate, the bar will either pull out of the concrete (shear failure in concrete along the plane of the deformations) or the concrete will split as a result of the radial stresses developed. The development length can be expressed by the equation:

$$l_d = f_y A_b / \pi d_b \tau_{avg} = f_y d_b / 4\tau_{avg} \quad (1)$$

Where τ_{avg} is the average bond stress that may be developed along the length l_d of the bar having diameter d_b. In practice, a number of factors contribute to development and the following empirical equation is adopted (ACI 318-14):

$$l_d = \frac{3 f_y d_b}{40} \frac{\Psi_t \Psi_e \Psi_s}{\sqrt{f_c'}\left(\frac{c_b + 40 A_{tr}/sn}{d_b}\right)} \quad (2)$$

Where f_c' is the concrete compressive strength (implying τ_{avg} is a function of $\sqrt{f_c'}$). The term in brackets accounts for concrete cover (c_b) and confinement (A_{tr}/sn), and the Ψ terms account for bar coating, size and placement, respectively. Finally, the 3/40 scalar is an empirical value calibrating the equation with experimental results for ASTM A615-compliant steel reinforcing bars.

Since titanium has a lower modulus and is therefore expected to exhibit greater slip for a given applied load, development equations need to be revised (or verified) for these new conditions. Indeed, development equations for GFRP bars, while accounting for the same concrete conditions, take a different empirical form (ACI 440.1R) requiring an iterative solution. Since GFRP is linear to failure, the problem is one of determining a development length, l_d, sufficient to develop the design stress, f_{fe}. The comparable Canadian code for GFRP-reinforced structures, CSA S806 (2002), also provides a development length equation

taking the same basic form as Eq. 2 although having an experimentally determined "bar surface profile factor", k_5, intended to account for bond characteristics of the bar. Based on the experience with GFRP, despite the lower material modulus, bond and development length are considered in a manner similar to steel. Nonetheless, comprehensive testing must be conducted to quantify a particular material's bond characteristics and strength for use in reinforced concrete structures. In this study, ASTM D7913 pull-out tests and ASTM A944 beam-end tests are used to compare the bond and development behaviours of 6Al-4V titanium and A615 steel; additional comparisons with GFRP reinforcement are provided in Platt (2018).

Geometric Properties of Titanium Reinforcing Bar

In this study three different heats of unannealed 6Al-4V titanium reinforcing bar provided by the same manufacturer are used. In addition, samples of Heat 1 were annealed to assess resulting changes in performance associated with annealing the rolled deformed bars. All A615 reinforcing bars reported come from the same heat. This section reports geometric properties for the bars used in subsequent mechanical characterization and bond tests. All bars are nominally #5 (US designation indicating a nominal diameter of 5/8 inch = 15.9 mm) bars. A sample of a bars used in this study is shown in Figure 1.

Cross section geometry

Cross sectional area was determined using the immersion method (Archimedes principle). The mass and volume of samples machined to lengths of 6.4 and 50.8 mm were determined. Nominal diameter was measured using a digital caliper and multiple measuring points around each sample. The resulting geometric properties are given in Table 1. Based on ASTM A615, the titanium bar size is marginally larger than a #5 bar which has a specified cross section area of 200 mm^2 and nominal diameter of 15.9 mm. Consistent with conventional practice, in all further discussion and calculation, the nominal cross sectional area of 200 mm^2 and the nominal value of bar diameter, d_b = 15.9 mm will be used unless noted otherwise.

Deformation geometry

Deformation geometry was assessed against the requirements of Section 7 of ASTM A615. With the exception of lug height in Heats 1 and 2, the 6Al-4V titanium bars are compliant with #5 ASTM A615 deformed reinforcing bar. ASTM A615 prescribes a minimum lug height of 0.71 mm. Lug heights are given in Table 1. Also shown in Table 1 is the rib ratio. R_r, defined as the ratio of the projected deformation normal to the bar axis to the product of the nominal bar diameter and deformation spacing (ACI 408.3R 2009):

$$R_r = \delta/s_r(1 - \Sigma B_n/360) \quad (3)$$

Where s_r is the spacing of deformations (lugs) along the bars and the remaining terms are described in Figure 1c. Although rib ratio is not a standard means of qualifying a reinforcing bar, based on the minimum bar deformation requirements prescribed by ASTM A615, the implied minimum permissible rib ratio is 0.048. Examples of titanium bars having R_r equal to 0.050 and 0.115, and a A615 bar having R_r = 0.079, are shown in Figure 1. The variation in Heats was the result of the 'learning curve'; the deformation geometry improved as the manufacturer produced subsequent heats. Heat 3 had quite large and well-defined lugs, easily meeting the requirements of ASTM A615.

Mechanical Properties of Titanium Reinforcing Bar

Tension tests of the as-received 6Al-4V titanium and A615 steel bars were conducted. Other than the material being titanium, the tests were compliant with ASTM A370 (including Annex A9) as referenced by ASTM A615. Yield was determined using the 0.2% offset method over a 50 mm instrument gauge length centred in a 200 mm specimen gauge length. The results are summarised in Table 1. In all calculations required for Table 1, measured material properties were used. Figure 2 shows representative stress-strain curves for all bars reported in this study. The 6Al-4V titanium material behaved as expected in terms of typical axial stress-strain behaviour (Figure 2), exhibiting a clear yield point and reasonable ductility. As expected, annealing the 6Al-4V had little effect on strength but improved the ductility somewhat.

ASTM D7913 Pull-out Testing

Pull-out tests have been widely used in evaluating the bond characteristics of reinforcement. This is primarily due to the ease and repeatability of the testing arrangement. However, the method, using a bonded length of only five bar diameters ($5d_b$) has been shown to overestimate the actual average bond stress for a corresponding full development length (Feldman and Bartlett 2005; Osofero et al. 2014). Thus, the test is more appropriate as an A-B comparison test rather than a test to establish a design parameter. The pull-out test, described in ASTM D7913 and shown in Figure 3, includes a length of reinforcing bar cast in a concrete cube with both ends exposed – the bar is bonded to the concrete over a length of only five bar diameters ($5d_b$; 80 mm in the specimen shown in Figure 3). The specimen is tested with one end of the bar loaded in tension while the other is monitored for slip relative to the concrete.

Concrete Material Properties

Three batches of ready-mix concrete were used in the pull-out and beam-end tests (described subsequently). The concrete mix designs and material properties are given in Table 2. A minimum batch size of 1.5 m^3 was mixed in every case to minimise the variability inherent in small ready-mix batches.

Pull-out Test Specimens

Table 3 summarises the 45 pull-out tests conducted for this test program. A minimum of 5 specimens of each titanium heat and a 'control' series of the same A615 bars were tested with each concrete batch in order to permit normalization of results. The #5 reinforcing bars were cast into 203 mm concrete cubes (Figure 3). All bars have a bonded region $5d_b$ = 80 mm long. The remaining embedded length is unbonded by placing it within a 19.2 mm I.D. (24.3 mm O.D.) GFRP tube (seen in Figure 3a).

Pull-out Test Set-up and Protocol

All pull-out tests were compliant with the method of ASTM D7913. A testing apparatus (Figure 3b) was fabricated to support the 203 mm concrete cubes while the embedded reinforcing bars were placed into concentric tension as to 'pull out' the reinforcement. The apparatus was designed to be mounted in a 600 kN capacity servo-hydraulic universal test machine and to be self-centering with respect to the axis of the pull-out test. Slip of the protruding unloaded end of the embedded bar was measured using a custom-

fabricated collar and linear position transducer (Figure 3c). The transducer has a range of 12 mm and a precision of 0.004 mm. A clip gage was installed on the loaded portion of the bar (seen in Figure 3b) to validate modulus data. Although continuous data was recorded during each test, ASTM D7913 defines "control" values of bond strength at specified slips of 0.05, 0.10, and 0.25 mm.

Pull-out Test Results

Using the ASTM D7913 test arrangement, the average bond stress, τ, over the $5d_b$ embedment is calculated as:

$$\tau = F/\pi d_b l_b \quad (4)$$

Where F is the tensile force applied to the reinforcement, d_b is the bar diameter, and l_b is the bonded length, equal to 80 mm in each case. Table 4 summarises the average results of all pull-out tests at ASTM D7913-prescribed values of slip of 0.05, 0.10, and 0.25 mm. All data is reported in terms of nominal bar geometry (i.e., d_b = 15.9 mm and A_b = 200 mm^2). Since the titanium bars are larger than the nominal dimensions (Table 1), the actual bond stress developed is lower in proportion to the difference in bar diameter (from 4% to 9% in this study) and the tensile stress in the bar at the same applied force is lower in proportion to the bar area (from 7.5% to 18% in this study).

Figure 4a summarizes the average observed bond stress-slip relationships for the ASTM D7913-prescribed values of slip reported in Table 4. Figure 5 shows the entire bond stress-slip relationship for all specimens tested. Superimposed in Figure 5 are the ASTM D7913-prescribed values of slip.

Bond stress is proportional to an exponential of concrete strength, $f_c'^n$, where n = 0.5 in ACI 318 practice [ACI 318-14 §25.4.2] and n = 0.66 in EC2 practice [EC2 §8.4]. In order to normalise the obtained data for concrete strength, bond stress is divided by $f_c'^{0.66}$ and plotted against slip in Figure 4b. The basis for selecting n = 0.66 is that it results in a better correlation for the steel pull-out tests. Since no other parameter apart from concrete strength was varied in the steel tests, it is expected that the normalised bond stress-slip relationships found for steel should be the same.

Effect of rib ratio, R_r

A single length of titanium bar from the beginning of the rolling of Heat 2 exhibited a considerable range of deformation geometry over an approximately 3 m length. This bar was designated “bar X” and was tested using Batch 2 concrete. Figure 6 shows the resulting ASTM D7913 backbone stress-strain curves for each segment of this bar having different rib ratio, R_r. Because this is a rolled bar, the area, diameter and rib ratio are related to the speed of rolling (and other issues); thus, as shown in Figure 6, the geometry at each station along the bar varies although remains compliant with a #5 bar.

Discussion and summary of pull-out test results

The nature of reinforcing bar bond to concrete is such that deformed bars will exhibit very similar patterns of bond stress-slip behaviour. This is evident in this study. Provided adequate deformations are provided, the bond-slip relationship is dominated by concrete behaviour. The bond performance of the titanium bars was similar to that of the steel bars and, as expected, clearly affected by the rib ratio. The results presented reinforce the necessity of meeting the ASTM A615-implied lower limit for the rib ratio, $R_r > 0.05$. In Figure 4b (normalised for concrete strength), Titanium Heat 1 ($R_r = 0.050$) demonstrates behaviour similar to A615 ($R_r = 0.079$) while Titanium Heat 3 ($R_r = 0.123$) demonstrates superior behaviour. The data shown in Figure 5 also shows similar behaviour for steel and titanium tests, provided R_r exceeds 0.05 (Figures 5a and c). Nonetheless, Figure 5 does show a greater degree of variation in titanium results. Finally, Figure 6 (all same Batch 2 concrete) also appears to indicate a threshold below which bond behaviour is poor, showing very low initial resistance to slip at Stations 6, 8 and 10, each having $R_r \geq 0.020$.

The implication of a similar bond-stress behaviour is that existing bond relationships for steel-reinforced concrete likely apply to the prototype titanium bars provided they meet the deformation requirements of ASTM A615 – the standard for which steel reinforcing bars, and therefore their bond characterisation – is calibrated.

ASTM A944 Beam-End Testing

A more representative method for assessing bond is the beam-end test described in ASTM A944; this has been adopted in many studies including numerous modified versions of the test. Like the pull-out test, the beam-end test is primarily an A-B comparison test, although the mechanics of the test result in a stress state, similar to that which occurs at the end of a simply supported beam. The longer embedment length of the beam-end test permits a better understanding of the development of the bar being tested. Indeed, the beam-end test can be designed to demonstrate full development, with the resulting failure mode being yield of the reinforcing bar.

The test matrix for the beam-end tests performed is summarised in Table 3. Three specimens of titanium Heats 2 and 3 were considered and a 'control' series of the same A615 bars were tested with each concrete batch to permit normalization of results.

Beam End Test Specimens

The beam-end test specimens are compliant with those described in ASTM A944 shown in Figure 7a. All specimens have the same dimensions, only the bonded length (l_b) of the embedded reinforcing bar is varied. The bonded lengths were selected as multiples of the basic tensile development length (l_d) of a #5 A615 bar having f_y = 413 MPa and $f_c' = 28$ *MPa*, determined from Eq 2 to be $l_d = 21.3d_b$ = 340 mm. The #5 reinforcing bars were cast into 229 x 660 x 622 mm concrete specimens. Bars have bonded lengths of $0.5l_d$, $1.0l_d$, or $1.5l_d$. The remaining embedded length is divided into two unbonded sections at either end of the specimen by placing it within 19.2 mm I.D. (24.3 mm O.D.) GFRP tubes.

Beam End Test Set-up and Protocol

All beam-end tests are compliant with the method of ASTM A944. The testing frame was designed around a large self-contained reaction frame. Load was applied concentrically to the bar using a 267 kN hollow-core hydraulic ram (Figure 7). The hydraulic pressure is used to calculate the applied load with a precision of 320 N. Slip is measured by implementing the same LVDT collar used in the cube pull-out tests (Figure 3c) having a precision of 0.004 mm which exceeds the 0.025 mm precision required by ASTM A944. Load was applied in 2.22 kN increments and instrument readings were taken from LVDTs at the loaded and free ends of the reinforcing bar at each load step.

Beam End Test Results

Using results from the ASTM A944 test arrangement, the average bond stress, τ, was calculated from Eq. 1. Table 5 summarizes the results. Typically, beam-end tests exhibit very little bar end slip before failure. In this study, the initial measurable slip (0.004 mm) and a second value (0.009 mm) are reported in addition to the measured slip at the ultimate capacity. In some cases, a brittle failure mode resulted in the ultimate slip not being recorded.

Discussion and Summary of Beam-End Test

The single A615 steel bar specimen demonstrated a bond pull-out failure in which the embedment was inadequate to develop the full capacity of the bar. In this case, with $l_b = 0.5l_d$, the bar was only able to develop $0.77f_y$ prior to pulling out from the beam end specimen. In contrast, the A615 specimens having $l_b = l_d$, were all able to develop more than $1.2f_y$ demonstrating the conservative nature of development length calculations (Eq. 2). When embedment length was increased to $l_b = 1.5l_d$, the bar was able to approach its ultimate capacity, exceeding $1.4f_y$, prior to failing. The results with A615 steel validate the concept of development length and the efficacy of the ASTM A944 test method as a basis of comparison. The tensile stress developed in the bars for the case of $1.0l_d$ = 340 mm was essentially the same for both steel and titanium bars (Table 5). At $1.5l_d$ = 511 mm, an approximately 10% greater stress was observed in the 6Al-4V titanium bars than in the A615 steel bars at the maximum load (Table 5). The capacity of the titanium bar beam-end tests appear to validate the use of Eq. 2 for the Heat 3 6Al-4V titanium bars tested. The 6Al-4V titanium has a yield strength 2.25 times that of the A615 steel (Table 1). Thus the straight bar development length calculated using Eq. 2 will be 2.25 times longer.

Prism Tension Tests

When a reinforcing bar embedded in concrete is loaded in tension, the adhesive component of the bond is the initial force transfer mechanism between bar and surrounding concrete followed by frictional slip. Both components quickly dissipate, replaced by the mechanical component of bond. Within the development length, the deformations will begin to bear into the concrete with resulting forces inclined

with respect to the bar axis (Collins and Mitchell 1997). The perpendicular component of this normal force produces a radially-oriented tension force in the surrounding concrete causing longitudinal splitting. The angled resultant force, however, engages the concrete surrounding the bar and will affect the rate at which force is transferred along the length of the bar. This, in turn, affects the transverse crack spacing and therefore crack widths. At a given bar strain, improved bond will result in smaller crack spacing and smaller crack widths.

Bond stress can be idealized by axially loading a single bar-reinforced concrete prism in tension. As the bar is loaded, 'primary' tensile cracks form in the concrete. At the crack locations, the tensile stress in the bar is described by $f_s = T/A_b$ and between these cracks, a portion of the load is transferred to the concrete through bond. As the bond forces accumulate, 'secondary' cracks develop between the 'primary' cracks; this process may repeat for 'tertiary' and 'quaternary' cracks if the bond-slip relationship is sufficiently stiff. No further cracks develop once the bond stress development between adjacent cracks is insufficient to develop the concrete tensile capacity of the concrete (Reis et al. 1964). Provided the concrete stress between the cracks is less than the tensile capacity of the concrete, the concrete and reinforcing are composite, resulting in lower reinforcing bar strains than at the cracks. This is known as "tension stiffening" (Collins and Mitchell, 1997). The bond stress is therefore proportional to the slope of the longitudinal reinforcing bar stress distribution:

$$df_s/dx = 4\mu/d_b \quad (5)$$

Where μ is the bond stress acting in the length dx. Since the tensile stress in the reinforcing bar is equal at each crack, the average bond stress between cracks, μ_{avg}, is also equal.

Prism Test Specimens and Test Method

Four 127 mm square x 1575 mm long specimens, each with a single #5 reinforcing bar cast through its centre with sufficient exposed length at either end to permit gripping in the testing frame were cast. As the embedded bar is loaded in tension, stress is transferred to the concrete by bond. The formation of resulting cracks are recorded including their locations, initiation loads, and a crack scope is used to accurately measure the width of the crack at predetermined load levels. Two of each bar type, A615 and

6Al-4V titanium (Heat 1) were tested. Material properties of the bars are given in Table 1. The prisms were cast with concrete from Batch 1 (Table 2). Direct tension tests were conducted in a 600 kN capacity servo-hydraulic load frame. Load was applied monotonically to develop a cracking history (primary, secondary, tertiary, etc.). Following this, the fully cracked specimens were loaded to 76, 125 and 173 kN and crack widths recorded. For such a test to provide meaningful data, the bars must remain elastic.

Prism Test Results

The applied load versus axial elongation (measured from machine crosshead displacement) of each specimen is shown in Figure 8. The initially soft response is a function specimen seating and initial test machine compliance. A summary of the crack development with monotonically increasing axial load, the crack widths and crack spacing are provided in Table 6. A photo of all four specimens following testing is shown in Figure 9. The following observations are made which reinforce previous discussions and observations:

1. Initial 'primary' cracking is a function of the concrete tensile capacity; the embedded bar, provided it is bonded to the concrete serves to control cracking but does not affect its initiation. In this study, the Batch 1 concrete exhibited initial cracking at a stress of 1.84 MPa = $0.35\sqrt{f'_c}$ (COV = 0.19). Within expected scatter for concrete, initial cracking is unaffected by the reinforcing bar material.
2. No further crack development was observed beyond an applied load of 50 kN (a reinforcing bar stress at the cracks of 250 MPa); beyond this load, only opening of existing cracks takes place.
3. Crack spacing is a function of bond behaviour – how efficiently does the bar transfer stress to the concrete at either side of a crack. The crack spacing for the steel bars is considered the control. In this study, the spacing was observed to be between 200 and 220 mm. The 6Al-4V titanium bars exhibited a 'softer' bond-slip relationship (see Figure 4) than the steel; thus the crack spacing is greater (about 320 mm).
4. Since the bars alone carry stress across the cracks, crack width is inversely proportional to bar axial stiffness, EA_b.

Discussion and Summary of Prism Test

For a given strain in a reinforced concrete prism, the resulting deformation is assumed to be the sum of the crack widths (strain between cracks is assumed to be negligible). To ensure good serviceability, ductility and continued adequate bond, it is desirable to have a large number of smaller cracks. However crack widths are a function of both bar modulus and bond characteristics. Crack width is inversely proportional to modular ratio E_{ti}/E_s, while spacing is inversely proportional to the stiffness of the initial bond-slip response. Therefore, the lower modulus 6Al-4V titanium bar exhibits larger crack widths at a given applied tensile force unless bond characteristics are improved proportionally.

Considering the limited tests reported here, these effects are evident. The load at which all cracks are developed (P = 50 kN) corresponds to a stress of 250 MPa or strain of 0.0013 for A615 steel and 0.0022 for 6Al-4V titanium – a difference proportional to the modular ratio, E_{ti}/E_s = 0.57. The crack spacing for the A615 specimens was approximately s = 215 mm, resulting in an average crack width of approximately 0.27 mm:

$$\frac{PL}{E_S A_b}\frac{s}{L} = \frac{50{,}000\ kN \times 1589\ mm}{200{,}000\ MPa \times 200\ mm^2}\frac{215\ mm}{1589\ mm} = 0.27\ mm \qquad (6)$$

The same calculation for the 6Al-4V titanium specimens having s = 319 mm results in an average crack width of approximately 0.70 mm, 260% greater. This difference results from a combination of the lower modulus and reduced bond stiffness of the 6Al-4V titanium. Assuming a modular ratio of 0.57, the ratio of titanium-to-steel bar bond stiffness is approximately 0.68 – a value similar to the same ratio of rib ratio, R_r = 0.050/0.079 = 0.63, for the bars tested.

A further comparison may be made of crack widths at comparable bar stress levels. In Table 6, the sum of measured crack widths and corresponding average specimen strain is reported at a bar stress level of $0.82f_y$ (applied forces of 76 kN and 173 kN, for steel and titanium, respectively). The total strain at comparable stress is expected to be 4 times greater for titanium than steel (i.e. $(E_s/E_{ti})(f_{yti}/f_{ys})$) and indeed, the observed strains are similar, if a bit greater. The greater crack spacing in the titanium specimens, however, result in proportionally greater average crack widths (Eq. 6) of 0.41 mm for A615 steel and 2.42

mm for 6Al-4V titanium – an increase of 590%. Once again, this difference results from a combination of the lower modulus and reduced bond stiffness of the 6Al-4V titanium.

It is hypothesized that were Heat 3 titanium bars available for this test, since the bond characteristics were improved, the crack spacing would decrease (likely to approximately 200 mm) and only the crack width would remain greater than that for steel.

Adoption and Potential Limitations of Titanium Reinforcing Bars

Material characteristics (in terms of elastic-plastic ductile behaviour) and bond performance of deformed 6Al-4V titanium bars having deformations similar to conventional steel reinforcing bars is similar to that of comparable steel bars. Nonetheless, use of 6Al-4V titanium bars will introduce serviceability concerns including larger crack widths at comparable bar stresses. This issue is exacerbated by the desire to use the higher strength titanium bars in a structurally efficient manner. Since the yield strength of titanium is on the order of 1000 MPa and the modulus is only 114 GPa, large deformations – on the order of four times greater than steel-reinforced concrete – are expected. Appropriate design philosophies needed to efficiently design with titanium reinforcing bars are proposed by Platt (2018).

Based on a preliminary evaluation, Platt (2018) identifies concerns associated with the fatigue performance of the prototype 6Al-4V titanium reinforcing bars tested. Platt (2018) also identified some concerns associated with the need to heat-bend titanium bars. These issues and the potentially larger deformations than in steel-reinforced structures make the use of titanium bars in seismic load resisting applications uncertain and in need of further investigation.

An additional area requiring further study is the use of 6Al-4V titanium bars for shear reinforcement in which complex interaction or reinforcing bars with cracked concrete provides resistance to shear force and limits the crack opening such that the aggregate interlock component of the concrete resistance remains engaged. A maximum strain in shear reinforcement to accomplish crack control is often reported to be 0.004 (ACI 440.1R-15; ACI Committee 426 1973).

Cost of titanium bars

The cost premium associated with the use of titanium material is a barrier that must be overcome. On a unit weight basis, 6Al-4V titanium bars are approximately 15 times more expensive than A615 bars and 5 times greater than solid stainless steel bars (Platt 2018; Triantafillou 2012). However design paradigm will affect the ultimate in-place cost of titanium bars. Platt (2018) conducted a preliminary study of the cost of using #5 6Al-4V titanium bars for bridge deck reinforcement (based on an earlier study by Triantafillou (2012) that addressed many bar materials, but not titanium). Depending on the design paradigm used, 6Al-4V reinforcing bars were estimated to cost between $430/m2 [of bridge deck constructed] and $1700/m2. A615 bars were estimated to cost $117/m2 and solid stainless steel bars were $294/m2. The typical bridge construction unit cost for medium span bridges using conventional A615 reinforcing bars (in 2010) is $989/m2 (Triantafillou 2012) thus the use titanium bars represents a significant cost premium. It is noted however that while 6Al-4V titanium may represent a raw material cost 40 times that of steel, with appropriate design, this equates to an in-place reinforcing bar cost about four times that of steel and an estimated total cost only 32% greater than an A615 steel-reinforced deck. Long term savings in maintenance for a non-corrosive deck can be leveraged to repay this initial cost premium.

Conclusions

This paper summarizes measured geometric and experimentally determined material and mechanical properties of prototype 6Al-4V titanium reinforcing bars and comparable properties of A615 steel bars. All bars are nominally #5 bars. Bond characteristics of the titanium bars were assessed through ASTM D7913 pull-out tests, ASTM A944 beam-end tests, and concrete prism tension tests. Both, the pull-out and beam-end tests are A-B tests that are best used to evaluate relative performance of reinforcing bars. The nature of reinforcing bar bond to concrete is such that deformed bars exhibited very similar patterns of bond stress-slip behaviour. Provided adequate deformations are provided, the bond-slip relationship is dominated by concrete behaviour. The bond performance of the 6Al-4V titanium bars was similar to that of A615 steel bars and, as expected, affected by the rib ratio. The results presented reinforce the need to

roll deformations such that the ASTM A615-implied lower limit for the rib ratio, $R_r > 0.05$ is satisfied. The implication of a similar bond-stress behaviour is that existing bond relationships for steel-reinforced concrete apply to titanium bars provided they meet the deformation requirements of ASTM A615 – the standard for which steel reinforcing bars, and therefore their bond characterisation – is calibrated. Both the pull-out and beam-end test results reinforce the conclusion that bond behaviour of 6Al-4V titanium bars having adequate deformations is essentially the same as that steel bars. The bond stresses, normalised to account for variation in concrete strength, are similar and the calculated development lengths are essentially in the ratio of yield strengths of the materials.

For a given strain in reinforced concrete, the resulting deformation is the sum of the crack widths. To ensure good serviceability, ductility and continued adequate bond, it is desirable to have a large number of small cracks. However crack widths are a function of both bar modulus and bond characteristics. Crack width is inversely proportional to modular ratio (E_{ti}/E_s), while spacing is inversely proportional to the stiffness of the initial bond-slip response. Therefore, the lower modulus 6Al-4V titanium bar will exhibit larger crack widths than comparable A615 steel bars unless bond characteristics are improved proportionally.

Acknowledgement

The research presented was sponsored by the Perryman Company. The findings and conclusions reported in this paper reflect the opinion of the authors and are not necessarily those of the Perryman Co. All testing was conducted in the Watkins Haggart Structural Engineering Laboratory at the University of Pittsburgh. The second author acknowledges the support of the Leverhulme Trust (UK).

References Cited

AASHTO (2014) *LRFD Bridge Design Specifications* (7th edition), American Association of State Highway and Transportation Officials.

ACI 318-14 (2014) *Building Code Requirements for Structural Concrete*, American Concrete Institute

ACI 408.3R-09 (2009) *Splice and Development Length of High Relative Rib Area Reinforcing Bars in Tension*, American Concrete Institute.

ACI 440.1R-15 (2005) *Guide for the Design and Construction of Structural Concrete Reinforced with FRP Bars*, American Concrete Institute.

ACI Committee 426 (1973) The Shear Strength of Reinforced Concrete Members, *Journal of the Structural Division* **99** (ST6) June 1973, pp 471-473.

Adkins, J. and George, W. (2017) Titanium Finds a Home in Civil Engineering, *Concrete International*, December 2017, pp 51-55.

ASTM A370-14 (2014) *Test Methods and Definitions for Mechanical Testing of Steel Products*, ASTM International.

ASTM A615-16 (2016) *Standard Specification for Deformed and Plain Carbon-Steel Bars for Concrete Reinforcement*, ASTM International.

ASTM A944-10 (2010) *Standard Test Method for Comparing Bond Strength of Steel Reinforcing Bars to Concrete Using Beam-End Specimens*, ASTM International.

ASTM C39-16 (2016) *Standard Test Method for Compressive Strength of Cylindrical Concrete Specimens*, ASTM International.

ASTM C496-11 (2011) *Standard Test Method for Splitting Tensile Strength of Cylindrical Concrete Specimens*, ASTM International.

ASTM D7913-14 (2014) *Standard Test Method for Bond Strength of Fiber-Reinforced Polymer Matrix Composite Bars to Concrete by Pullout Testing*, ASTM International.

Collins, M. P., and Mitchell, D. (1997). *Prestressed concrete structures*. Toronto: Response Publications.

CSA S806-12 (2012) *Design and construction of building components with fibre-reinforced polymers*. Canadian Standards Association.

EuroCode 2 (EC2) (2004) BS-EN 1992 *Design of concrete structures*

Feldman, L. R., and Bartlett, F. M. (2005). Bond strength variability in pullout specimens with plain reinforcement. *ACI Structural Journal*, **102**(6), 860.

Higgins, C. (2015) Titanium Reinforcing for Strengthening RC Bridges, *International Bridge Conference*, Pittsburgh, PA, June 2015.

Higgins, C. Knudtsen, J. Amneus, D. and Barker, L. (2017) Shear and Flexural Strengthening of Reinforced Concrete Beams with Titanium Alloy Bar, *Proceedings of the 2nd World Congress on Civil, Structural, and Environmental Engineering (CSEE'17)*, Barcelona, Spain, Apr. 2017.

Higgins, C. Amneus, D. and Barker, L. (2015) Methods for Strengthening Reinforced Concrete Bridge Girders Containing Poorly Detailed Flexural Steel Using Near-Surface Mounted Metallics, Report No. *FHWA-OR-RD-16-02*, Oregon Department of Transportation, Salem, OR, 138 pp.

Osofero, A. I., Corradi, M., and Borri, A. (2014). Experimental Study of Bond Strength between Titanium Bar and Lime-Based Mortar. *Journal of Materials in Civil Engineering*, 04014182.

Platt, S. (2018) *Development of Titanium Reinforcing Bars for Concrete and Masonry*, Doctoral dissertation, University of Pittsburgh.

Platt, S. and Harries, K.A. (2018) Study of Galvanic Corrosion Potential of NSM Titanium Reinforcing Bars, *Case Studies in Construction Materials* **9**, e00175.

Reis, E. E., Mozer, J. D., Bianchini, A. C. and Kesler, C. E. (1964). Causes and control of cracking in concrete reinforced with high strength steel Bars—A review of research, *T. and A. M. Report No. 261*, University of Illinois, IL.

Triantafillou. L (2012) Cost Comparison of Corrosion Resistant Reinforcing Steel – Deployment Considerations, *FHWA Office of Infrastructure Research and Development* as updated by Wong, W. (2014) http://www.dot.state.fl.us/statematerialsoffice/structural/meetings/crrb/12_deployment.pdf (retrieved 15 August 2015).

Table 1 Geometric and material properties of #5 bars used in this study (COV in brackets).

property	unit	ASTM A615 Steel	6Al-4V titanium			
			Heat 1	Heat 1 annealed	Heat 2	Heat 3
		Geometric Properties				
bar area, A_b	mm^2	200[1]	223 (0.041)		215 (0.016)	236 (0.010)
diameter, d_b	mm	15.9[1]	16.85 (0.021)		16.55 (0.008)	17.35 (0.005)
density	kg/m^3	7700[1]	4466		4433	4407
weight	kg/m	1.556[1]	0.995		0.953	1.040
average lug height[2], δ	mm	0.92	0.62		0.49	1.37
rib ratio[3], R_r (Eq. 3)		0.079	0.050		0.033	0.123
		Material Properties (ASTM A370)				
yield strength, f_y	MPa	464 (0.046)	1055 (0.009)	1044 (0.009)	1090 (0.009)	999 (0.005)
tensile strength, f_u	MPa	740 (0.022)	1092 (0.008)	1082 (0.011)	1133 (0.009)	1054 (0.003)
modulus[4], E	GPa	177 (0.076)	102 (0.034)	107 (0.037)	101 (0.059)	94.3 (0.051)
ultimate elongation		0.257 (0.206)	0.161 (0.158)	0.176 (0.067)	0.093 (0.121)	0.084 (0.042)

[1] nominal value

[2] ASTM A615 requires lug height ≥ 0.71 mm; Ti Heats 1 and 2 do not meet this requirement

[3] ASTM A615 implies a requirement $R_r \geq 0.05$; Ti Heat 2 does not meet this requirement

[4] modulus was determined using external clip gages. These values are lower than typically assumed values of 200 GPa for steel and 114 GPa for titanium

Table 2 Concrete mix design and material properties.

	batch 1	batch 2	batch 3
Type I/II cement	294 kg/m^3		
fine aggregate	688 kg/m^3 SSD		
3/8 in. gravel	1015 kg/m^3 SSD		
class C fly	73.6 kg/m^3 (20% cm replacement)		
AE: Axim AE 260	190 ml/m^3		
WR: Axim 1000N	5.56 kg/m^3		
water	167 kg/m^3	157 kg/m^3	165 kg/m^3
w/c	0.45	0.43	0.45
target slump	140 mm		
target air	6.7%		
unit weight	2227 kg/m^3		
28 day compressive strength (ASTM C39)	f_c' = 28.3MPa (COV = 0.02)	f_c' = 43.6 MPa (COV = 0.004)	f_c' = 43.3 MPa (COV = 0.05)
28 day split cylinder strength (ASTM C496)	2.42 MPa = 0.46$\sqrt{f_c'}$ (COV = 0.11)	3.43 MPa = 0.52$\sqrt{f_c'}$ (COV = 0.07)	2.57 MPa = 0.39$\sqrt{f_c'}$ (COV = 0.12)

Table 3 Bond test matrix indicating number of specimens tested.

			ASTM D7913 pull-out test	ASTM A944 beam end test		
bonded length, l_d			80 mm	$0.5l_d$ = 170 mm	$1.0l_d$ = 340 mm	$1.5l_d$ = 511 mm
#5 bars	heat	concrete				
ASTM A615	-	batch 1	5	-	-	-
		batch 2	5	1	3	3
		batch 3	5	-	3	-
6Al-4V titanium	1	batch 1	10	-	-	-
	1 annealed	batch 2	5			
	2	batch 2	5	-	3	3
	3	batch 3	10	-	3	3
Ti bar X	2	batch 2	5	-	-	-

Table 4 Summary of ASTM D7913 pull-out test results (COV in brackets).

		ASTM A615 Steel			6Al-4V Titanium Heat 1	6Al-4V Titanium Heat 1 annealed	6Al-4V Titanium Heat 2	6Al-4V Titanium Heat 3
R_r		0.079			0.050	0.050	0.033	0.123
concrete		batch 1	batch 2	batch 3	batch 1	batch 2	batch 2	batch 3
samples	n	5	5	5	10	5	5	10
		initiation of slip						
load	kN	8.74 (0.13)	7.17 (0.39)	11.9 (0.73)	12.2 (0.25)	6.43 (0.19)	5.40 (0.32)	10.1 (0.25)
bar stress	MPa	43.7	35.9	59.7	61.0	32.1	27.0	50.5
	$1/f_y$	0.09	0.08	0.13	0.06	0.03	0.02	0.05
bond stress	MPa	2.20	1.81	3.00	3.07	1.62	1.36	2.54
		0.05 mm slip						
load	kN	16.2 (0.11)	22.1 (0.29)	19.4 (0.43)	17.7 (0.20)	12.0 (0.24)	12.7 (0.37)	28.5 (0.19)
bar stress	MPa	81.0	110	97.2	88.2	60.1	63.3	143
	$1/f_y$	0.17	0.24	0.21	0.08	0.06	0.06	0.14
bond stress	MPa	4.08	5.56	4.89	4.44	3.02	3.19	7.19
		0.10 mm slip						
load	kN	21.0 (0.12)	29.1 (0.22)	23.6 (0.39)	20.4 (0.22)	15.8 (0.24)	16.1 (0.37)	36.9 (0.17)
bar stress	MPa	105	146	118	102	78.9	80.3	184
	$1/f_y$	0.23	0.31	0.25	0.10	0.08	0.07	0.18
bond stress	MPa	5.30	7.33	5.95	5.13	3.97	4.04	9.28
		0.25 mm slip						
load	kN	29.6 (0.07)	45.9 (0.13)	33.0 (0.34)	27.2 (0.19)	25.1 (0.21)	23.7 (0.30)	50.5 (0.14)
bar stress	MPa	148	229	165	136	126	118	252
	$1/f_y$	0.32	0.49	0.36	0.13	0.12	0.11	0.25
bond stress	MPa	7.46	11.6	8.31	6.84	6.33	5.96	12.7
		maximum load						
load	kN	45.3 (0.10)	73.7 (0.08)	66.4 (0.10)	43.6 (0.15)	52.1 (0.16)	38.6 (0.22)	65.8 (0.13)
slip	mm	1.34 (0.24)	1.23 (0.09)	1.52 (0.43)	1.49 (0.12)	1.70 (0.14)	1.48 (0.21)	1.17 (0.20)
bar stress	MPa	227	368	332	218	260	193	329
	$1/f_y$	0.49	0.79	0.71	0.21	0.25	0.18	0.33
bond stress	MPa	11.4	18.6	16.7	11.0	13.1	9.73	16.6
$l_d = f_y d_b / 4\tau$	mm	162	100	111	375	316	438	239

Table 5 Summary of ASTM A944 beam end test results (COV in brackets).

		ASTM A615 Steel				6Al-4V Titanium Heat 2	6Al-4V Titanium Heat 3	6Al-4V Titanium Heat 2	6Al-4V Titanium Heat 3
R_r		0.079				0.033	0.123	0.033	0.123
concrete		batch 2	batch 2	batch 3	batch 2	batch 2	batch 3	batch 2	batch 3
embedment, l_b		$0.5l_d$ 170 mm	$1.0l_d$ 340 mm	$1.0l_d$ 340 mm	$1.5l_d$ 511 mm	$1.0l_d$ 340 mm	$1.0l_d$ 340 mm	$1.5l_d$ 511 mm	$1.5l_d$ 511 mm
samples	n	1	3	3	3	3	3	3	3
		0.004 mm slip							
load	kN	28.9	41.7 (0.03)	73.4 (0.18)	122 (0.03)	38.5 (0.43)	89.0 (0.13)	115 (0.35)	136 (0.06)
bar stress	MPa	145	209	367	612	193	445	575	682
	$1/f_y$	0.31	0.45	0.79	1.32	0.18	0.45	0.53	0.68
average bond stress	MPa	3.39	2.46	4.32	4.80	2.27	5.23	4.51	5.35
		0.009 mm slip							
load	kN	55.6	86.7 (0.08)	95.6 (0.16)	133	79.3 (0.21)	106 (0.05)	142 (0.02)	139 (0.05)
bar stress	MPa	278	434	478	667	397	530	708	697
	$1/f_y$	0.60	0.93	1.03	1.44	0.36	0.53	0.65	0.70
average bond stress	MPa	6.53	5.10	5.63	5.23	4.67	6.24	5.55	5.47
		maximum load							
load	kN	71.2	113 (0.02)	119 (0.01)	131 (0.04)	119 (0.07)	114 (0.01)	145 (0.02)	145 (0.04)
slip	mm	0.02	0.04 (1.04)	-	0.01 (0.05)	0.03 (0.71)	-	0.01 (0.43)	-
bar stress	MPa	356	563	593	656	593	571	727	727
	$1/f_y$	0.77	1.21	1.28	1.41	0.54	0.57	0.67	0.73
average bond stress, τ	MPa	8.35	6.63	6.98	5.15	6.98	6.72	5.70	5.70
$l_d = f_y d_b / 4\tau$	mm	219	279	264	359	625	592	757	694

Table 6 Crack history, widths and spacing for prism tension tests.

		ASTM A615 Steel		Heat 1 6Al-4V Titanium	
		Fe1	Fe2	Ti1	Ti2
bar yield stress	MPa	464	464	1055	1055
load at first crack	kN	30.7	22.3	29.8	35.6
stress in concrete[2] at first crack	MPa	$1.91 = 0.36\sqrt{f'_c}$	$1.39 = 0.26\sqrt{f'_c}$	$1.86 = 0.35\sqrt{f'_c}$	$2.22 = 0.42\sqrt{f'_c}$
stress in bar[1] at first crack	MPa	$154 = 0.33f_y$	$112 = 0.24f_y$	$149 = 0.14f_y$	$178 = 0.17f_y$
load at 2nd crack	kN	35.6	25.9	31.6	36.7
stress in bar[1] at 2nd crack	MPa	$178 = 0.38f_y$	$130 = 0.28f_y$	$158 = 0.15f_y$	$183 = 0.17f_y$
load at 3rd crack	kN	35.6	25.9	35.3	39.7
stress in bar[1] at 3rd crack	MPa	$178 = 0.38f_y$	$130 = 0.28f_y$	$177 = 0.17f_y$	$199 = 0.19f_y$
load at 4th crack	kN	36.1	25.9	39.4	41.1
stress in bar[1] at 4th crack	MPa	$181 = 0.39f_y$	$130 = 0.28f_y$	$197 = 0.19f_y$	$205 = 0.19f_y$
load at 5th crack	kN	43.1	38	-	-
stress in bar[1] at 5th crack	MPa	$215 = 0.46f_y$	$190 = 0.41f_y$	-	-
load at 6th crack	kN	49.2	39.3	-	-
stress in bar[1] at 6th crack	MPa	$246 = 0.53f_y$	$197 = 0.42f_y$	-	-
load at 7th crack	kN	-	44.5	-	-
stress in bar[1] at 7th crack	MPa	-	$223 = 0.48f_y$	-	-
sum of crack widths at $0.82f_y$[1]	mm	1.52	1.27	8.13	5.59
approximate strain at $0.82f_y$[1]		0.001	0.0008	0.0051	0.0035
average crack spacing (COV)	mm	227 (0.18)	204 (0.22)	318 (0.16)	320 (0.21)

[1] stress calculated using nominal bar area: $A_b = 200$ mm^2 and experimentally determined f_y
[2] stress calculated using gross concrete area: $A_g = 16000$ mm^2 and $f_c' = 28.3$ MPa

a) ASTM A615 bar (left) having R_r = 0.079 and Heat 1 titanium bars (right) having R_r = 0.050

b) titanium bar deformation pattern (Station 2 of "Bar X" shown having R_r = 0.115)

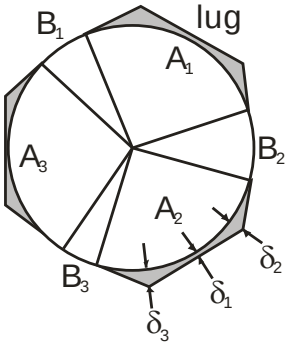

c) bar deformation geometry (Eq. 3)

Figure 1 Samples of reinforcing bars used in this study and definition of lug geometry.

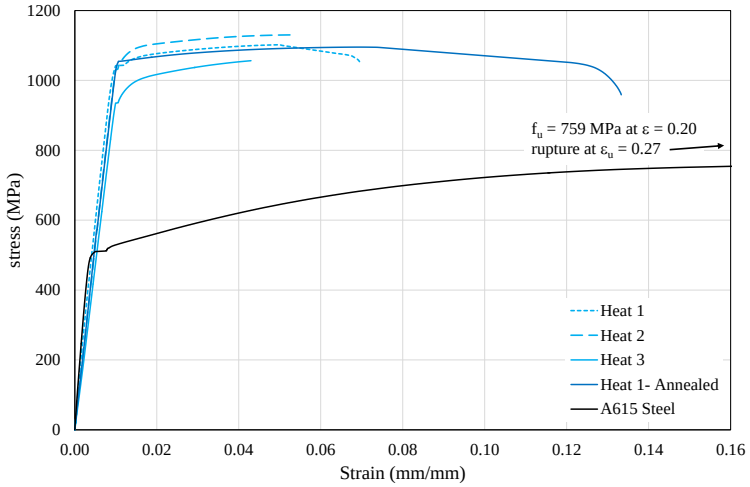

Figure 2 Representative titanium and steel stress-strain curves.

a) titanium reinforcing bar with GFRP tube bond breaker

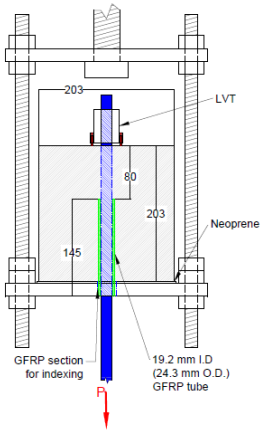

b) test apparatus

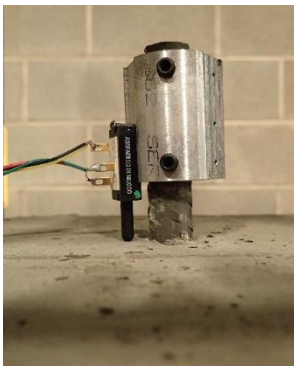

c) collar and transducer for measuring slip of embedded bar at unloaded end

Figure 3 ASTM D7913 Pull-out test specimens and test arrangement.

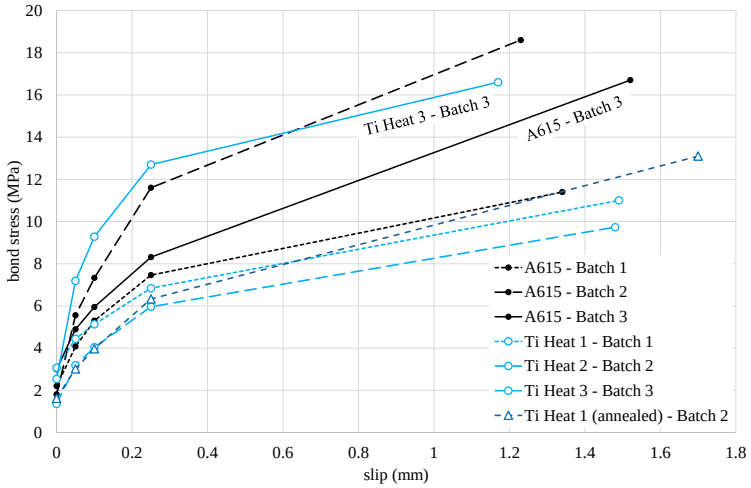

a) experimentally determined relationships

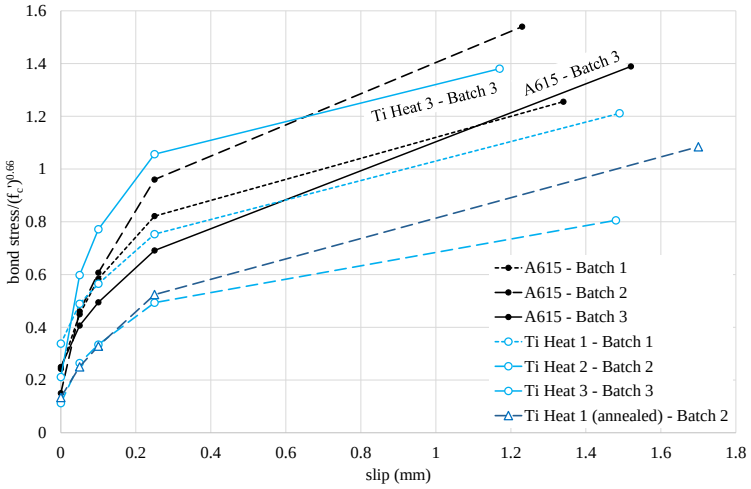

b) normalised for concrete strength

Figure 4 Average bond stress-slip relationships.

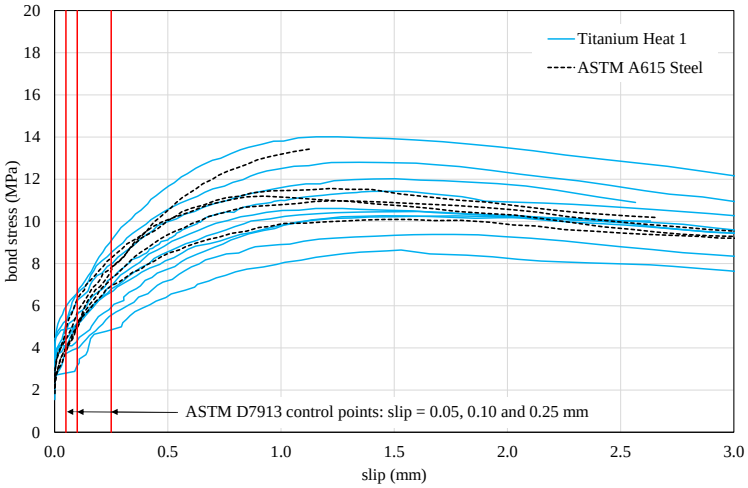

a) Batch 1 concrete (Ti Heat 1)

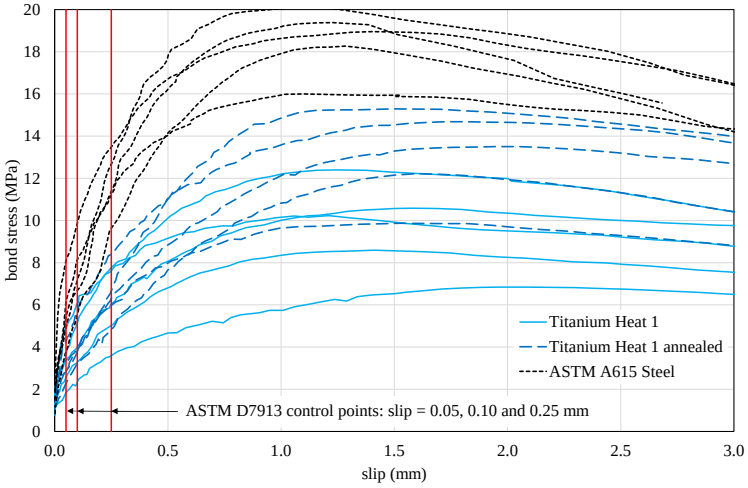

b) Batch 2 concrete (Ti Heat 2 and Heat 1 annealed)

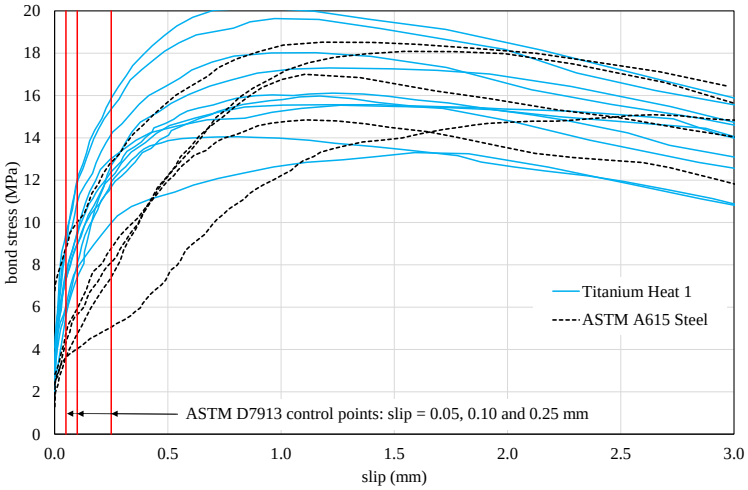

c) Batch 3 concrete (Ti Heat 3)

Figure 5 Complete average bond stress-slip relationships.

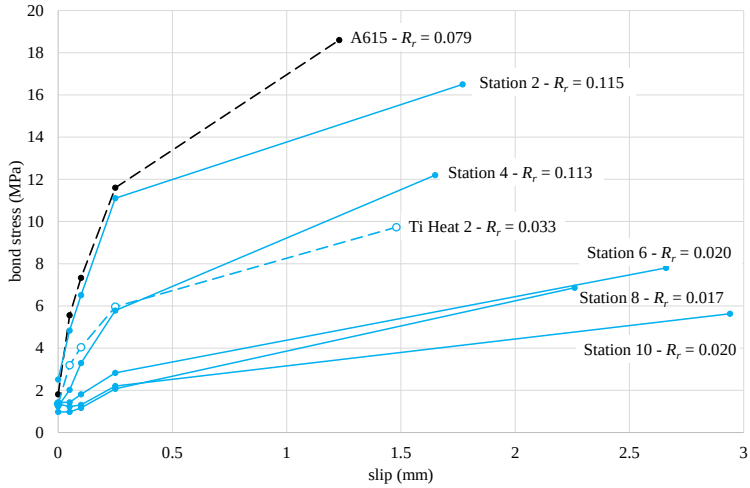

Bar X Station	A_b (mm^2)	d_b (mm)	lug height (mm)	R_r
2	232	17.2	1.28	0.115
4	228	17.0	1.28	0.113
6	208	16.3	0.36	0.020
8	206	16.2	0.28	0.017
10	213	16.5	0.33	0.020
Heat 2 average	215	16.6	0.49	0.033

Figure 6 Bond stress-slip relationships for “bar X” having varying rib ratio [all Batch 2 concrete].

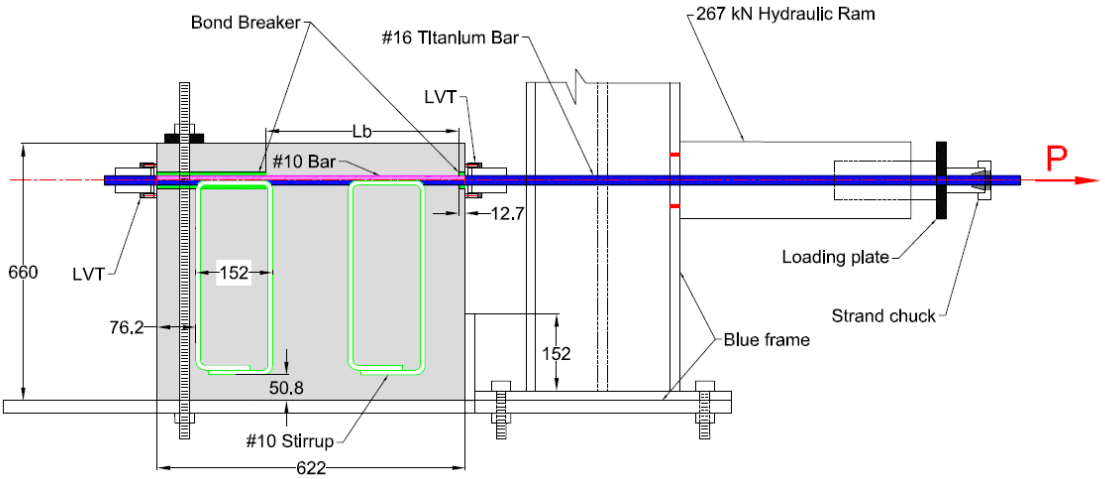

a) schematic fixture for beam end test (after ASTM A944)

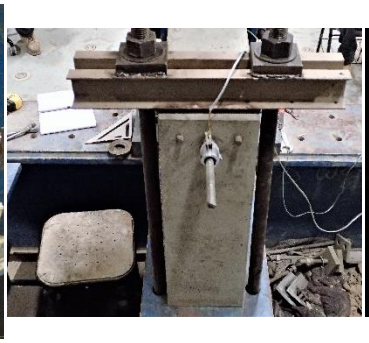

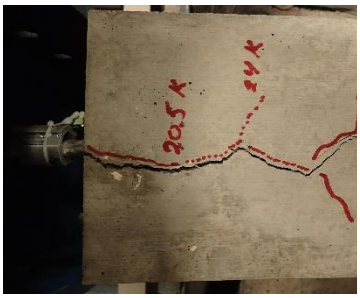

b) photo of apparatus c) free end d) loaded end during testing

Figure 7 ASTM A944 beam end test set-up.

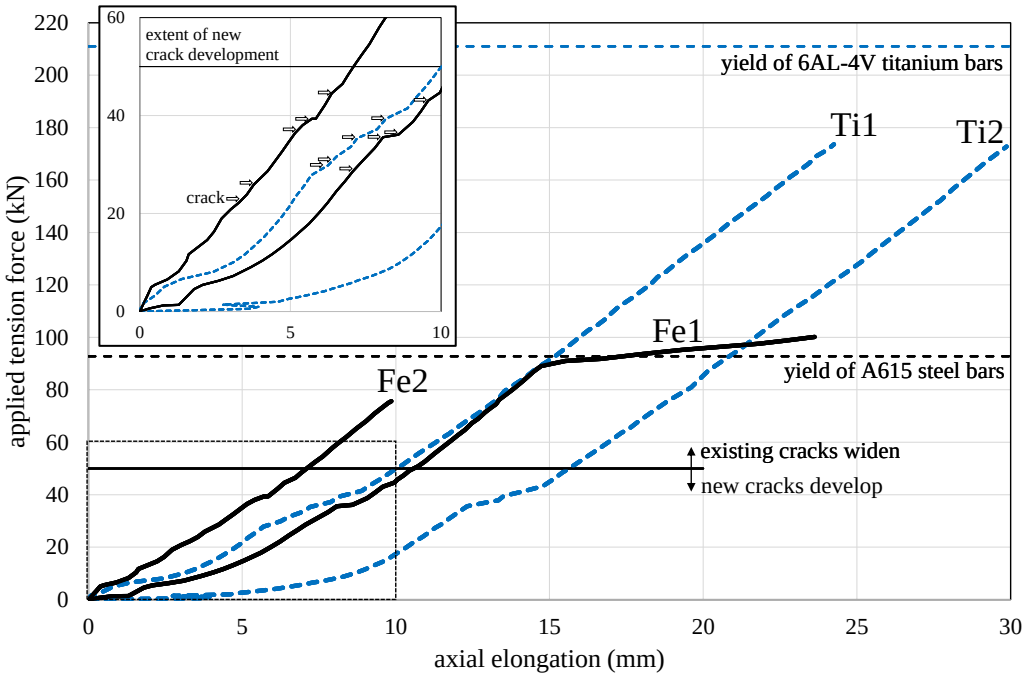

Figure 8 Prism specimen load-deformation curves.

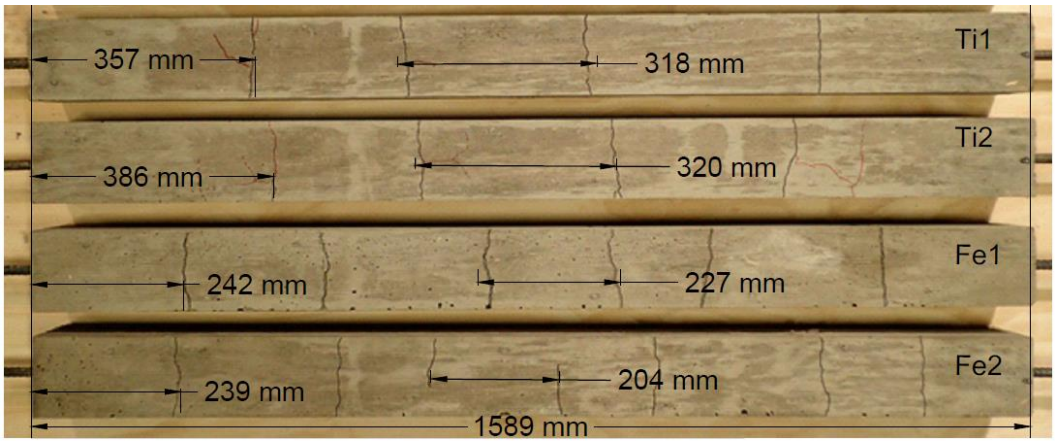

Heat 1 Titanium

Heat 1 Titanium

A615 Steel

A615 Steel

Figure 9 Prism specimens following testing showing crack patterns.